Rev.Adv.Mater.Sci. 21(2009) 44-56

SURFACE SEGREGATION ANISOTROPY AND THE EQUILIBRIUM SHAPE OF ALLOY CRYSTALS

Paul Wynblatt[1] and Dominique Chatain[2]

[1]Department of Materials Science and Engineering, Carnegie Mellon University, Pittsburgh PA 15206, USA
[2]CINAM-CNRS, Campus de Luminy, 13288 Marseille Cedex 9, France

Received: December 20, 2008

Abstract. A model of anisotropy of surface energy, resulting from surface segregation, has been used to calculate the equilibrium crystal shape (ECS) of FCC alloy crystals. The parameters of the model, including (a) surface energy differences between pure solvent and solute, (b) the regular solution constant, and (c) solute strain energy, have been varied in order to evaluate their effects on the ECS. Whereas the model predicts that the ECS of pure metals should only display {111} and {100} facets, the effects of segregation can produce several new facets, e.g. at {110}, {311}, {331}, and {210} orientations. In particular, new cusps in the γ-plot can only appear if the solute strain energy parameter has finite values. Also, it has been found that for any pair of orientations, the ratio of surface energies displays a minimum at the temperature corresponding to the crossover in adsorption for those two surface orientations. These crossovers occur over a limited temperature range, and new cusps that are deep enough to produce new facets on the ECS also tend to occur in that restricted temperature range. Some comparisons with experimentally determined ECSs of alloy crystals are provided, and show that the model can provide valuable though qualitative guidance for experiments.

1. INTRODUCTION

Models of surface segregation that are applicable to any surface orientation have been available for some time [1-3]. Recently, these models have been extended to allow calculation of the energy of the segregated surfaces based on a representation of the surface energy as the surface excess grand potential [4]. Thus far, such models have only been developed for FCC alloys. Although they can be applied in principle to the surfaces of other crystal structures, we will confine our attention in this paper to the surfaces of FCC alloy crystals, for which some experimental information is available [5-7].

The equilibrium crystal shape (ECS) of a material is directly related to its surface energy anisotropy. In particular, it is possible to apply the Wulff construction [8] to extract the ECS from polar plots of the surface energy anisotropy, i.e. from so-called γ-plots. In order for facets to occur on the ECS cusps must be present in the γ-plot. However, the existence of cusps in the orientation dependence of interfacial energy is a necessary, but not a sufficient condition for the appearance of facets on the ECS [9]. In order for a facet to occur on the ECS, not only must a cusp in surface energy be present at the facet orientation, but the cusp must be deep enough to penetrate the inner envelope of Wulff planes that define the ECS. Thus, models that provide a means of calculating the energy of segregated surfaces, as a function of their orientations, can be used to obtain the ECS of alloy crystals.

Some preliminary results of this type have been published previously [4]. In this paper we provide the results of more comprehensive calculations, in which the model parameters have been varied in a systematic manner, in order to identify the conditions that produce highly faceted equilibrium crystal shapes. This issue is important because the anisotropy of pure FCC metal is relatively weak, and leads to equilibrium crystal shapes that are

Corresponding author: Paul Wynblatt, e-mail: pw01@andrew.cmu.edu

bounded mainly by curved surfaces, with a few facets occurring at low index orientations (e.g. Pb [10-12], Au [13-15], and Cu [16]). In contrast, the few studies that have been performed on the ECS of alloys have reported highly faceted shapes (e.g. in the Cu-O [5], Cu-Bi [6], and Pb-Bi-Ni [7] systems).

2. MODEL OVERVIEW

Consider a semi-infinite FCC crystal, which consists of atoms located on the lattice points of a stack of planes of orientation (*hkl*) terminating at the surface. The Miller indices of the surface plane must be chosen such that $h \geq k \geq l$, and be reduced to the lowest integers. (*hkl)* planes in the crystal are numbered by an index *i*, where $i = 1$ identifies the surface plane. It is also necessary to define a second index, *j*, which counts the planes from any given plane *i*. The maximum value of *j* is denoted by J_{max}, and represents the farthest plane containing nearest neighbors of atoms in the *i*-th plane. It is defined by $J_{max} = (h+k)/2$ when *h*, *k*, and *l*, are all odd, and $J_{max} = (h+k)$ for mixed odd and even *h*, *k*, and *l*. The indices *i* and *j* are explained in greater detail in the papers of Lee and Aaronson [1,2].

We consider an FCC binary A-B regular substitutional solid solution in which the solute species is taken to be component B. For convenience, we also assume that the solute (B) corresponds to the segregating species. The composition of the *i*th atom plane will then have the usual regular solution form:

$$\ln\frac{x^i}{1-x^i} = \ln\frac{x}{1-x} - \frac{\Delta H^i_{seg}}{RT}, \tag{1}$$

where x^i and x are the atomic fractions of component B in the *i*-th atomic plane and in the bulk, respectively, and ΔH^i_{seg} is the enthalpy of segregation to the *i*-th plane, which includes both chemical and elastic energy terms.

We write the surface energy using an approach first employed to describe segregation to the surface of a liquid [17]. In this approach, the surface energy is expressed as the interfacial excess grand potential:

$$\gamma = e^S - Ts^S - \mu_A\Gamma_A - \mu_B\Gamma_B, \tag{2}$$

where e^S is the excess internal energy per unit area of surface, s^S is the excess surface entropy per unit area of surface, μ_A and μ_B are the chemical potentials, and Γ_A and Γ_B are the adsorptions of the respective components.

We now proceed to write each of the terms in Eq. 2, in the regular solution approximation, with an added elastic energy term. Each atom plane is taken to consist of *n* atoms per unit area (*n* will of course depend on the Miller indices (*hkl*) of the terminating plane). The internal energy for the surface terminated crystal is written:

$$\begin{aligned}
e^S = {} & \frac{nz^i}{2}\sum_{i=1}^{N+1}\left[\left(x^i\right)^2\varepsilon_{BB} + 2x^i\left(1-x^i\right)\varepsilon_{AB} + \left(1-x^i\right)^2\varepsilon_{AA}\right] - \Delta E^i_{el}x^i \\
& + \frac{n}{2}\sum_{i=2}^{J_{max}}\sum_{j=1}^{i-1} z^j\left[x^i x^{i-j}\varepsilon_{BB} + x^i\left(1-x^{i-j}\right)\varepsilon_{AB} + \left(1-x^i\right)x^{i-j}\varepsilon_{AB} + \left(1-x^i\right)\left(1-x^{i-j}\right)\varepsilon_{AA}\right] \\
& + \frac{n}{2}\sum_{i=1}^{J_{max}}\sum_{j=1}^{J_{max}} z^j\left[x^i x^{i+j}\varepsilon_{BB} + x^i\left(1-x^{i+j}\right)\varepsilon_{AB} + \left(1-x^i\right)x^{i+j}\varepsilon_{AB} + \left(1-x^i\right)\left(1-x^{i+j}\varepsilon_{AA}\right)\right] \\
& + \frac{n}{2}\sum_{i=J_{max}+1}^{N+1}\sum_{j=1}^{J_{max}} z^j\left[x^i x^{i-j}\varepsilon_{BB} + x^i\left(1-x^{i-j}\right)\varepsilon_{AB} + \left(1-x^i\right)x^{i-j}\varepsilon_{AB} + \left(1-x^i\right)\left(1-x^{i-j}\right)\varepsilon_{AA}\right. \\
& \left. + x^i x^{i+j}\varepsilon_{BB} + x^i\left(1-x^{i+j}\right)\varepsilon_{AB} + \left(1-x^i\right)x^{i+j}\varepsilon_{AB} + \left(1-x^i\right)\left(1-x^{i+j}\right)\varepsilon_{AA}\right] \\
& - \frac{nz(N+1)}{2}\left[(x)^2\varepsilon_{BB} + 2x(1-x)\varepsilon_{AB} + (1-x)^2\varepsilon_{AA}\right] \\
& + \frac{n}{2}\sum_{i=N-J_{max}+2}^{N}\sum_{j=N+2-i}^{J_{max}} z^j\left[x^i x^{i+j}\varepsilon_{BB} + x^i\left(1-x^{i+j}\right)\varepsilon_{AB} + \left(1-x^i\right)x^{i+j}\varepsilon_{AB} + \right. \\
& \left.\left(1-x^i\right)\left(1-x^{i+j}\right)\varepsilon_{AA} - \left\{(x)^2\varepsilon_{BB} + 2x(1-x)\varepsilon_{AB} + (1-x)^2\varepsilon_{AA}\right\}\right],
\end{aligned} \tag{3}$$

where the nearest neighbor bond energies ε_{AA} and ε_{BB} are computed from the surface energies of the pure components and ε_{AB} from the regular solution constant, ω, of the AB binary alloy ($\omega = \varepsilon_{AB} - [\varepsilon_{AA} + \varepsilon_{BB}]/2$); ΔE_{el}^{i} is the bulk elastic energy of a solute atom that is relieved in layer *i* (discussed in more detail later); z^i is the number of nearest neighbors of an atom in the *i*-th plane which also lie in the *i*-th plane; z^j is the number of nearest neighbors of an atom in the *i*-th plane which lie in the *j*-th plane (such that the total coordination of an atom is given by $z = z^i + \sum_{j=1}^{J_{max}} z^j$); and *N* is the total number of planes which have a composition different from the bulk. *N* is taken to be several multiples of J_{max}, (3 or 4 times J_{max} is generally sufficient to ensure that the *N*-th plane composition has essentially converged to that of the bulk). The first term in Eq. (3) represents the energy of in-plane bonds for all planes up to the (*N+1*)-th; the second term calculates the energy of interface-directed bonds in planes *i=2* to J_{max} that are connected to atoms in planes closer to the interface; the third term accounts for the energy of bonds in the first J_{max} planes that point away from the interface; the fourth term represents the energy of out-of-plane bonds for planes $i = J_{max}+1$ to *N+1*; the fifth term subtracts the energy of *N+1* planes of bulk composition; and finally the sixth term reflects internal energy contributions arising in the region of the surface composition profile where the composition excursion associated with surface segregation connects to the bulk composition of the crystal. When *N*, the total number of atom planes that have a composition different from the bulk, is chosen to be large enough, the final term makes a negligible contribution to the total internal energy of the surface.

The surface excess entropy per unit area is given by:

$$s^S = -nR\sum_{i=1}^{N}\Big[x^i \ln x^i + (1-x^i)\ln(1-x^i) - x\ln x - (1-x)\ln(1-x)\Big]. \quad (4)$$

The chemical potentials of the components in a binary regular solution may be expressed as:

$$\mu_A = \frac{z}{2}\Big[2x^2\omega + \varepsilon_{AA}\Big] + RT\ln(1-x), \text{ and}$$
$$\mu_B = \frac{z}{2}\Big[2(1-x)^2\omega + \varepsilon_{BB}\Big] + RT\ln x, \quad (5)$$

and the adsorptions of the two components are given by:

$$\Gamma_A = n\sum_{i=1}^{N}(x - x^i), \text{ and } \Gamma_B = n\sum_{i=1}^{N}(x^i - x). \quad (6)$$

Substituting Eqs. (3) to (6) into Eq. (2) gives the surface energy, and minimizing this energy with respect to the atom fraction of each plane *i* yields expressions for the equilibrium atom fractions of solute in each atom plane. The expressions for the equilibrium atom fractions will have the form of Eq. (1), in which the heat of segregation of the *i-th* atom plane is given by:

$$\Delta H_{seg}^{i} = 2\omega\Bigg[zx - z^i x^i - \sum_{j=1}^{J_{max}} z^j x^{i+j} - \sum_{j=1}^{i-1} z^j x^{i-1} - \frac{1}{2}\sum_{j=i}^{J_{max}} z^j\Bigg] - \frac{1}{2}(\varepsilon_{BB} - \varepsilon_{AA})\sum_{j=i}^{J_{max}} z^j - \Delta E_{el}^{i} \quad (7a)$$

for $i \le J_{max}$, i.e. planes with less than the bulk coordination, and by:

$$\Delta H_{seg}^{i} = 2\omega\Bigg[zx - z^i x^i - \sum_{j=1}^{J_{max}} z^j\left(x^{i+j} + x^{i-j}\right)\Bigg] - \Delta E_{el}^{i} \quad (7b)$$

for the planes $N \ge i > J_{max}$.

It should be noted that the equation for the composition of a given plane *i*, obtained by substituting ΔH_{seg}^{i} into Eq. (1), is transcendental and must be solved for the equilibrium plane composition by numerical methods. Once the equilibrium plane compositions are known, they can be used in Eqs. (3) to (6) combined in Eq. (2) to compute the surface energy.

As will be shown below, the solute elastic strain energy term in the model plays an important role in the effects of segregation on the surface energy anisotropy, and hence on the predicted ECS of alloys. In order to describe how the solute strain energy is relieved in each atom plane, it is necessary to use a method for defining the change in solute strain energy with distance from the surface. This is accomplished by adopting a variation of the model of Eshelby [18] for the change in elastic energy of a misfitting sphere with distance from a surface due to Steigerwald *et al*. [3]. The solute strain energy relieved in atom plane *i*, ΔE_{el}^{i}, is written:

$$\Delta E_{el}^{i} = E(\infty)\exp\Big[-101\left(h^i / r_B\right)^{1.53}\Big], \quad (8)$$

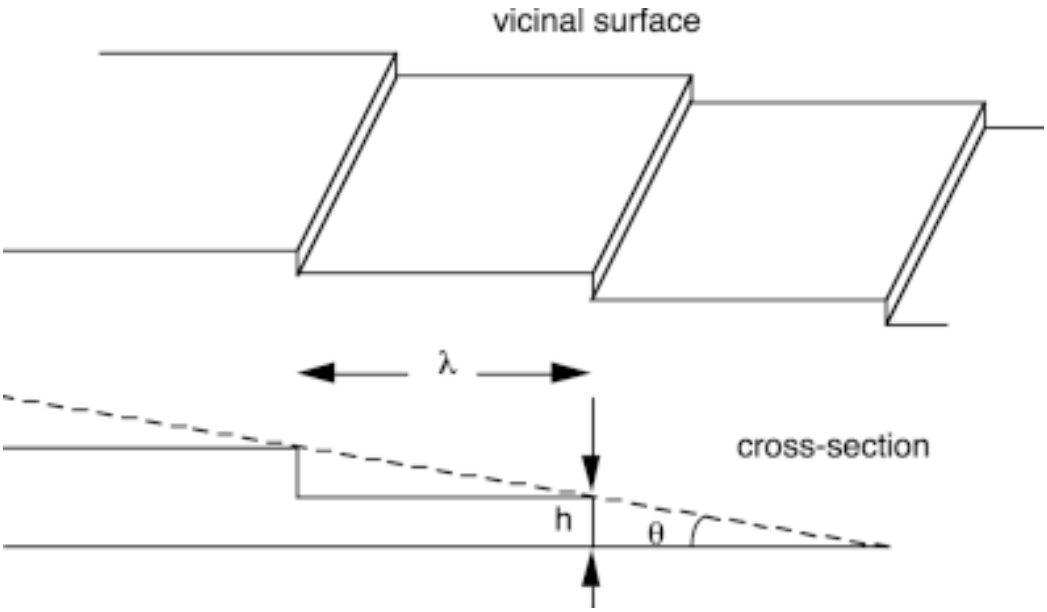

Fig. 1. Schematic of a vicinal surface consisting of terraces and steps, in perspective in upper panel and in cross-section in lower panel. θ is the angle between the vicinal surface and the terrace orientation, *h* is the step height and λ the step spacing.

where h^i is the distance of the *i*-th layer from the plane $i = 1$, r_B is the radius of a solute atom and $E(\infty)$ is the elastic strain energy of a solute atom in the bulk [19]:

$$E(\infty) = \frac{24\pi K_B G_A r_A r_B (r_A - r_B)^2}{4G_A r_A + 3K_B r_B}. \quad (9)$$

In Eq. (9), K_B is the bulk modulus of the solute species *B*, G_A is the shear modulus of the solvent, and r_A and r_B are is the radii of solvent and solute atoms, respectively. For $h^i = 0$, Eq. (18) leads to $\Delta E_{el}^i = E(\infty)$, i.e. all of the strain energy associated with the *B*-atom in the bulk is relieved at the surface.

3. RELATION BETWEEN NEAREST NEIGHBOR BOND MODEL AND ECS

We begin by describing the relationship between the surface energy calculated by the nearest neighbor bond model (NNBM) and surface orientation in a pure crystal. This is illustrated here for vicinal surfaces, i.e. surfaces that consist of terraces and steps, but no kinks, as shown in Fig. 1.

The energy of such a surface can be written:

$$\gamma(\theta) = \gamma_0 \cos\theta + \frac{\varepsilon}{h}\sin\theta, \quad (10)$$

where θ is the angle between the vicinal surface and the terrace orientation, γ_o is the energy of the terrace orientation, ε is the step energy (energy per unit length), and *h* is the step height. A general expression for γ(θ) would include additional terms representing step-step interactions [12], but those are absent in the NNBM. Eq. (10) has the same form as the polar coordinate equation of a circle that passes through the origin:

$$r = 2c\cos\alpha\cos\theta + 2c\sin\alpha\sin\theta, \quad (11)$$

where *c* is the radius of the circle, and α is the angle made by the circle diameter to the reference axis. Thus, a 2-dimensional (2D) slice through the γ-plot of a pure FCC metal, computed by the NNBM (for example by the model of Lee and Aaronson [1,2]) for orientations corresponding to vicinal surfaces, will consist of circular segments. This result is illustrated in Fig. 2, which is a 2D γ-plot of vicinal surfaces corresponding to the <110> zone of FCC crystals. Fig. 2a shows that the arcs which make up the γ-plot indeed correspond to circles passing through the origin. Fig. 2b displays the corresponding 2D ECS obtained by the Wulff construction, which shows that the NNBM predicts a completely faceted ECS consisting only of {111} and {100} type facets (for a temperature of absolute zero). It should be mentioned that, by analogy with the 2D result described here, it can be shown that the complete

Table 1. Parameters used for the various trials to investigate ECSs.

Trial	x(solute)	$\Delta\gamma$ (mJ/m^2)	ω (J/mol)	$E(\infty)$(J/mol)	New facets
NiAu (base)	0.001	0.54	2485	36400	{110}
ECS1	0.001	0	0	2*36400	none*
ECS2	0.001	0	0	1.5*36400	none*
ECS3	0.05	0	2485	0	no new cusps*
ECS4	0.02	0	2485	0.25*36400	{311} {331}
ECS5	0.02	0	3000	0	no new cusps*
ECS6	0.005	0	3000	0.5*36400	{311} {110} {210}
ECS7	0.001	0.81	2485	1.5*36400	{311} {110} {210}
ECS8	0.001	0.81	2485	0.25*36400	{311} {110} {331} {210}
ECS9	0.003	0.81	2485	0.25*36400	{311} {110} {210}
ECS10	0.001	0.81	5000	0.25*36400	{311} {110} {331} {210}

* "none" indicates that new cusps are formed on the γ-plot, but are not deep enough to lead to the formation of new facets; whereas "no new cusps" indicates that no cusps develop at orientations other than {111} and {100}.

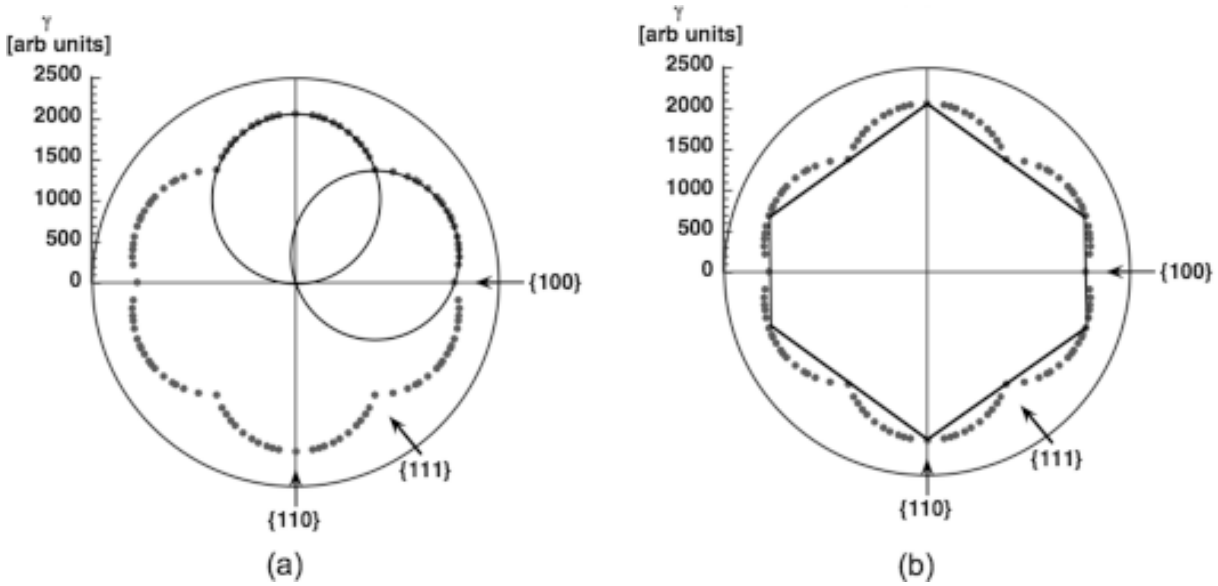

Fig. 2. 2D polar plots of surface energy (γ-plots) along the <110> zone of an FCC crystal. The points represent surface energies calculated at specific surface orientations by the NNBM. (a) The circles illustrate that the γ-plot is made up of arcs of circles that pass through the origin. (b) The corresponding ECS obtained by the Wulff construction is shown.

3D γ-plot obtained from the NNBM is bounded by surfaces that consist entirely of segments belonging to spheres that pass through the origin.

Two features that are present in the model of the surface energy of segregated crystals can modify the results described above for pure crys-

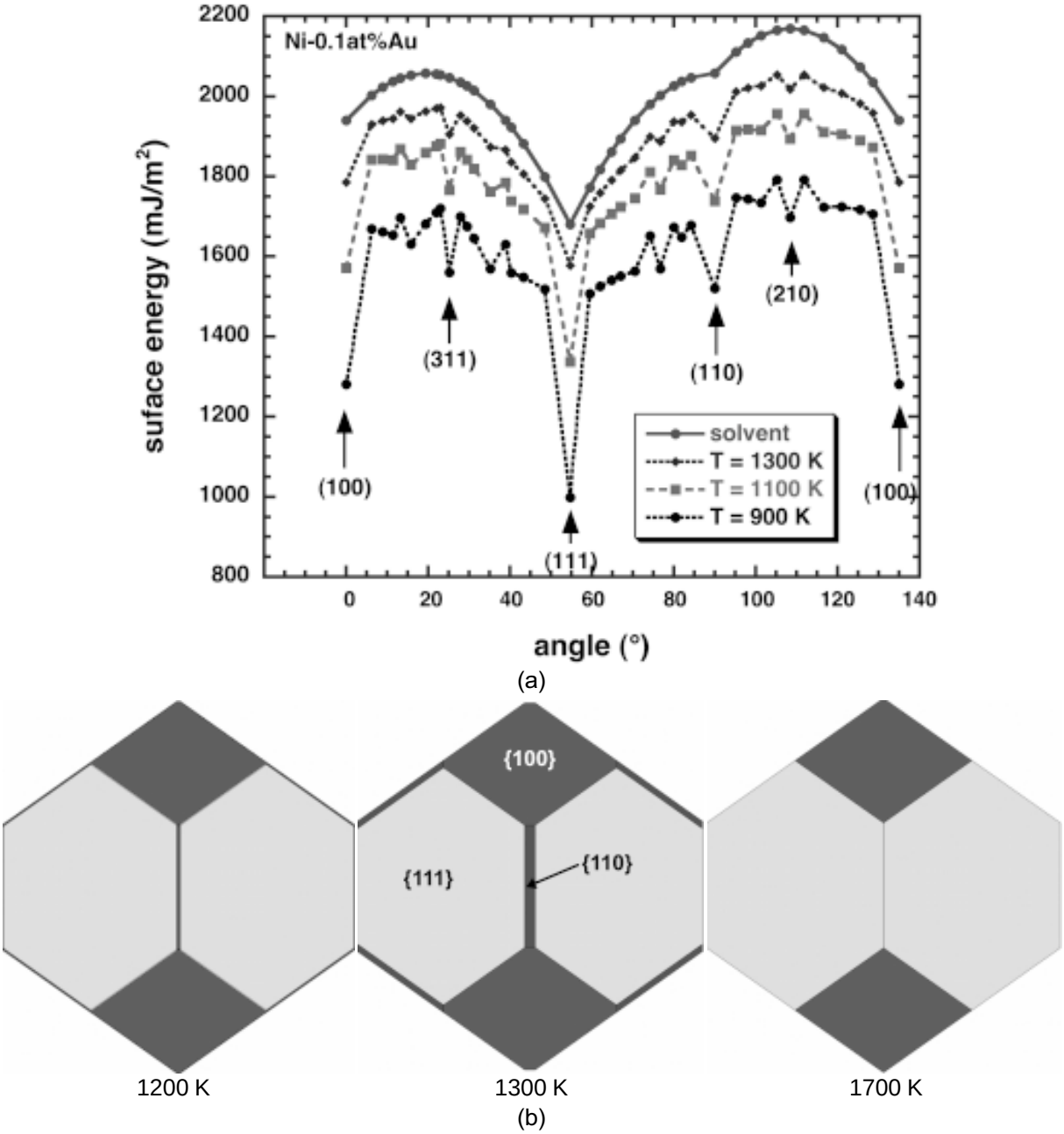

Fig. 3. (a) Surface energy variation with orientation around the edge of the stereographic triangle. Curves are shown for the pure solvent, and for a Ni-0.1at%Au alloy at three temperatures. (b) ECS of Ni-0.1at.%Au as viewed along <110> at three temperatures, showing appearance, growth and eventual disappearance of the new {110} facets as temperature is lowered [4].

tals: (a) surface segregation can modify the surface energy in an anisotropic manner, and (b) the segregation model is not just a NNBM, since it also contains elastic strain energy terms which introduce non pairwise contributions into the energy expression. These features will turn out to be important in the results described below.

4. RESULTS AND DISCUSSION

4.1. Results of model calculations

In a previous study, we reported the predictions of the segregation model for the ECS of Ni alloys dilute in Au [4] where Au is known to segregate strongly to the surface [3,20]. The model

parameters used for Ni-Au are given in the first row of Table 1. Here we use these values of the parameters as a base, and proceed to modify them over a broad range of values, as summarized in Table 1.

Fig. 3a shows the calculated variation in surface energy for the pure Ni solvent, as well as that for a Ni-0.1at.%Au alloy at three temperatures, as the surface orientation is varied around the edges of the standard stereographic triangle (i.e., from (100) to (111) to (110) and finally back to (100)). As can be seen, the overall anisotropy of surface energy (i.e. the ratio of the maximum to minimum energies) is considerably increased by Au segregation to the Ni-alloy surface. The cusps that existed in pure Ni at {111} and {100} are greatly deepened. In addition, however, significant new cusps in surface energy are produced at {311}, {331}, {110}, and {210} orientations. In order to construct the ECS based on information such as that given in Fig. 3a, we have made use of the Wulffman software [21]. Plots of the ECS of Ni-0.1%Au are shown for three temperatures in Fig. 3b. It can be seen that thin {110} facets occur on the ECS at the highest temperature (1700K). These facets are somewhat enlarged as the temperature is lowered to 1300K, but finally disappear at 1200K. This indicates that not all of the new cusps are sufficiently deep to penetrate the inner envelope of Wulff planes that define the ECS.

The appearance and disappearance of facets with changing temperature is related to the relative changes in surface energy for different orientations. This issue is addressed in Fig. 4. Fig. 4a shows the calculated variation in adsorption with temperature for the surface orientations associated with surface energy cusps in Fig. 3a. It can be seen that crossovers in adsorption occur, i.e. for any pair of orientations there is a temperature at which the adsorption is the same. One important feature associated with the crossover temperature is that it corresponds to a minimum in the ratio of surface energy for these two orientations, as shown in Fig. 4b for the case of the energy ratio of selected surface orientations to the {111} surface. This interesting finding, first reported in [4], may be stated as follows: *for any pair of orientations, the ratio of the surface energies displays a minimum at the temperature corresponding to the crossover in adsorption for those two surface orientations, i.e. where the two adsorptions are identical*. The minima in the energy ratios of Fig. 4b all occur within a finite temperature interval, which ranges from about 1250K to 1400K for the case of Ni-0.1at.%Au. The important point made by this figure is that cusps at orientations other than {111} and {100} are not deep enough to penetrate the envelope of Wulff planes, and thus appear as facets on the ECS, except where their energy is relatively close to the minima shown in that figure. As a result, facets at orientations other than {111} and {100} tend to appear first (upon temperature decrease) near the high end of the temperature interval where minima in energy ratios occur, and then disappear upon further cooling once these ratios become too large.

One other general result is worthy of note. Cusps at orientations other than {111} and {100} orientations only occur if the solute elastic strain energy is finite. For the set of parameters defined as ECS5 in Table 1, in which $E(\infty)$ has been set to zero and the bulk solute concentration has been raised to 2 at.%, so as to maintain a high level of segregation comparable to Ni-0.1at.%Au, Fig. 5a shows that no new cusps (i.e. other than {111} and {100}) are observed. However, when the solute elastic strain energy is increased gradually from zero to a temperature of 1700K, with other parameters held constant, several new cusps appear. This example shows that unless some contribution of solute strain energy is present in the enthalpy of segregation, no new cusps will appear in the dependence of surface energy on orientation. *Thus, we conclude that it is necessary to have some non-pairwise bond contribution in the enthalpy of segregation for new cusps to appear.*

Fig. 6 summarizes some of the more interesting cases listed in Table 1 where new facets appear on the ECS. For all possible parameter combinations, new facets only appear close to the temperature interval where crossovers occur in adsorption. Above and below that interval, only {111} and {100} facets are present on the ECS. New facets observed in Fig. 6 include {311}, {110}, {331}, and {210}. Although small cusps occur at other orientations, they never deepen sufficiently to penetrate the inner envelope of the Wulff planes that define the ECS.

4.2. Comparison with experimental results

In pure Pb and Au, experiments have shown [10-15] that the ECS consists predominantly of curved surfaces, with small facets at {111} and {100} orientations. However, measurements of the ECS can only be performed at high temperatures, in order to avoid prohibitively long equilibration times. At

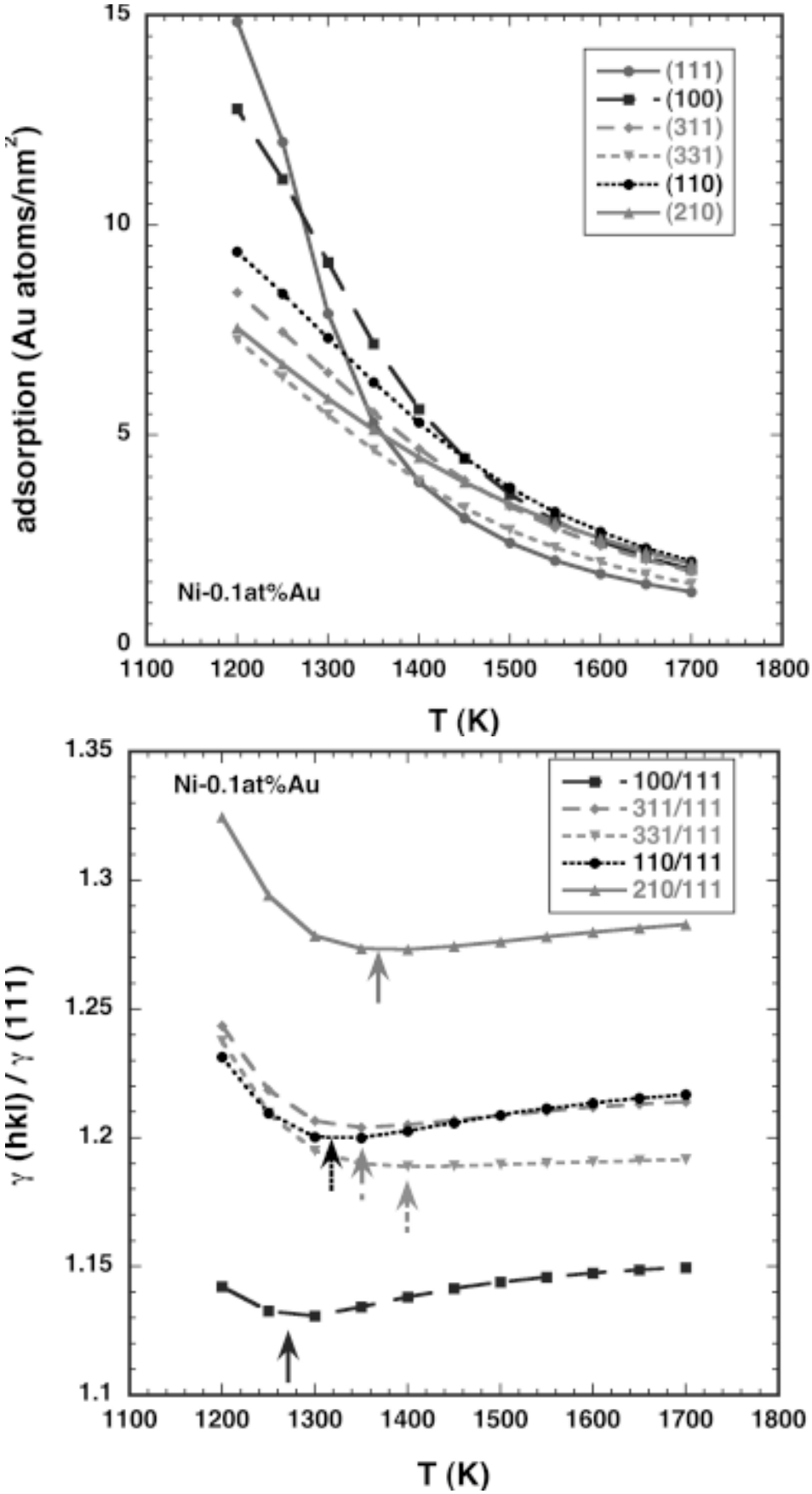

Fig. 4. (a) Adsorption vs. temperature for six orientations in Ni-0.1at.%Au. (b) Ratio of surface energies of five of the orientations in (a) to the energy of the (111) orientation vs. temperature; temperatures at which minima occur are indicated by arrows.

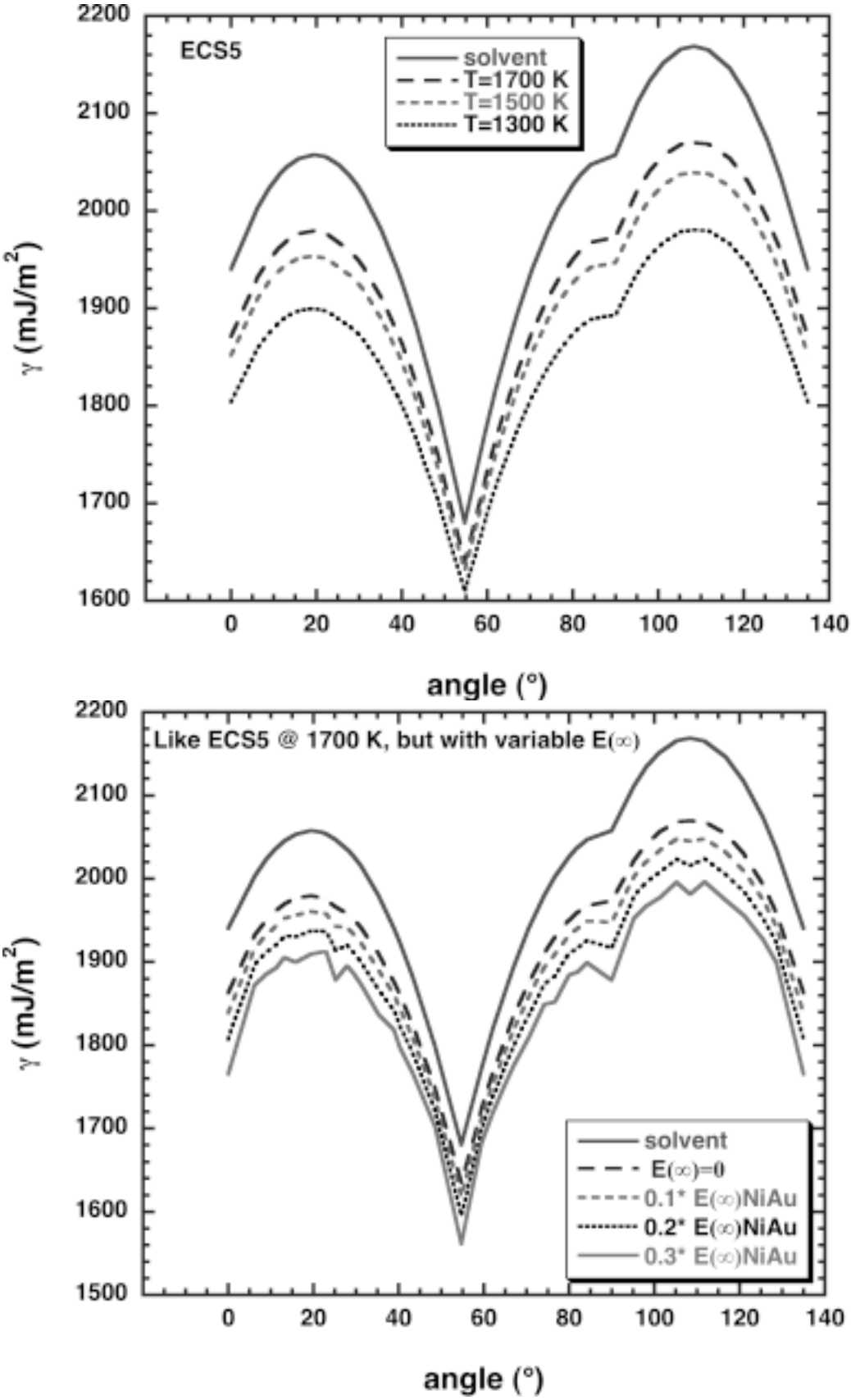

Fig. 5. Surface energy variation with orientation around the edge of the stereographic triangle. (a) Curves are shown for the pure solvent, and for parameters corresponding to ECS5 in Table 1, at three temperatures. (b) Curves are shown for parameters corresponding to ECS5 at 1700K, but with increasing value of $E(\infty)$.

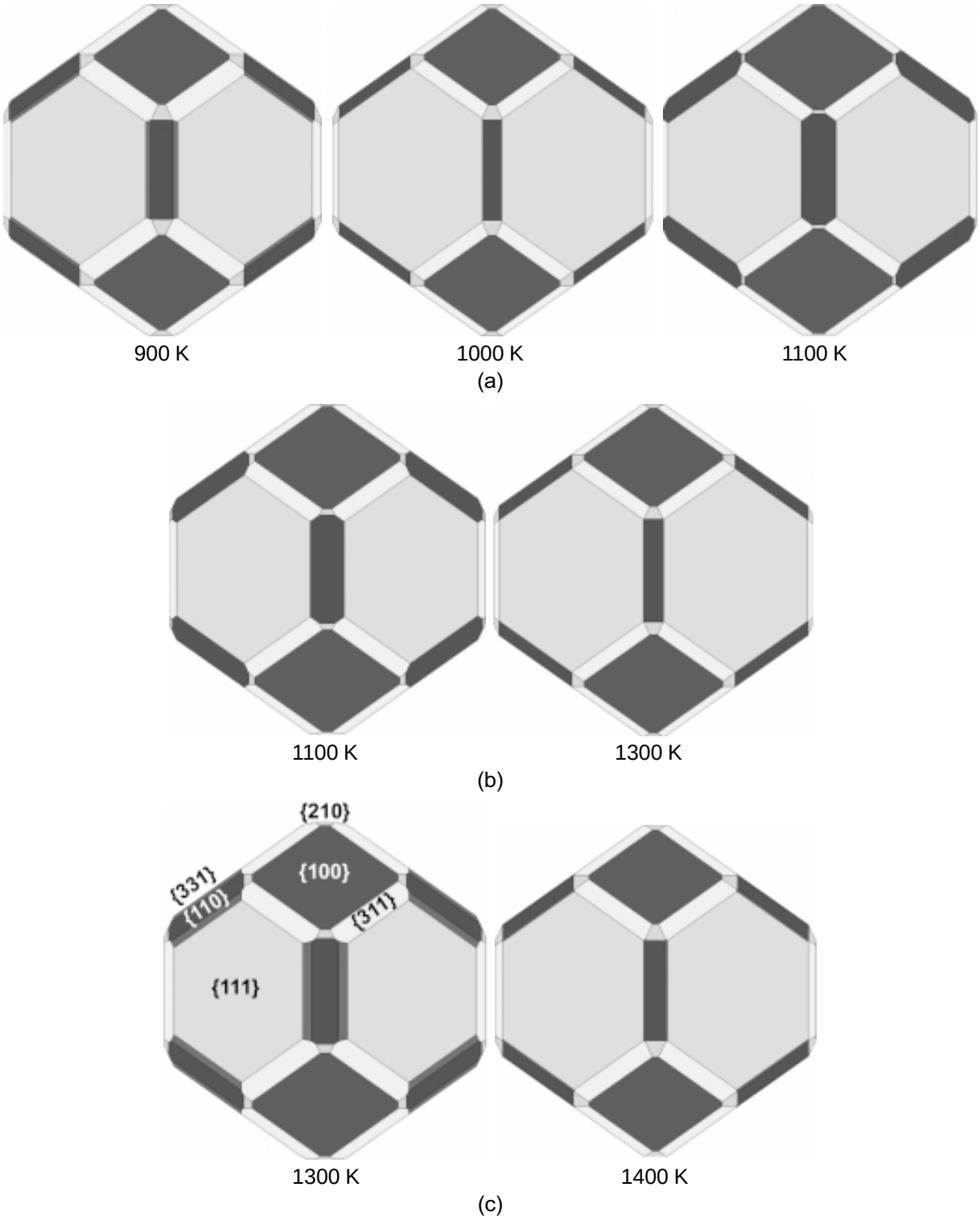

Fig. 6. ECSs (as viewed along a <110> direction) obtained under different conditions identified in Table 1: (a) ECS8, (b) ECS9, and (c) ECS10, at the temperatures indicated. Facets are labeled in (c) at 1300K.

these high temperatures, curved surfaces appear on the ECS due to roughening of certain surface orientations as a result of entropy effects. However, the present model for the surface energy of

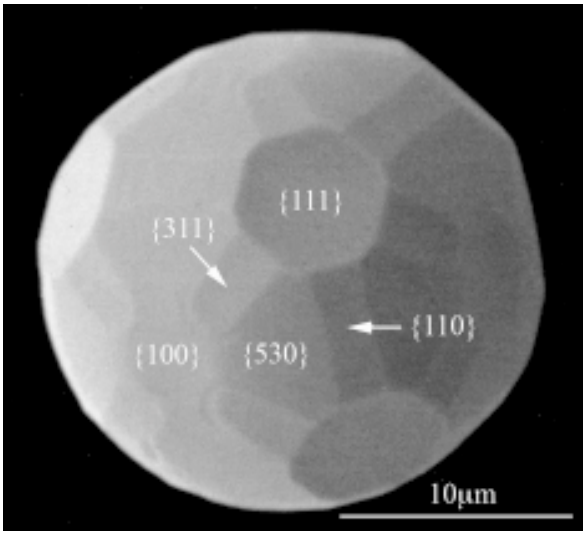

(a)

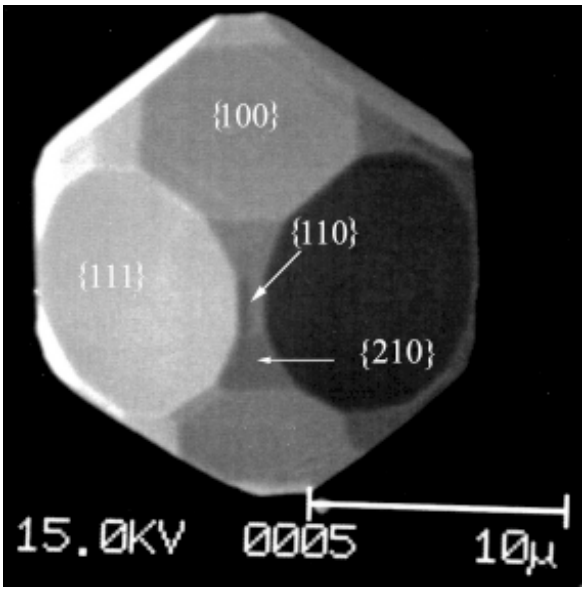

(c)

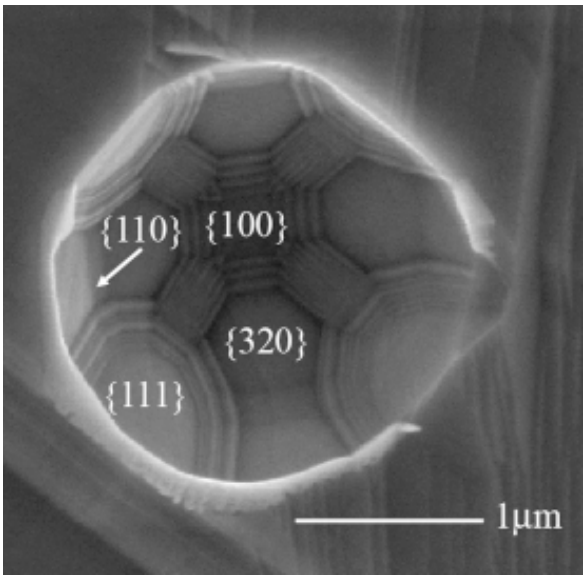

(b)

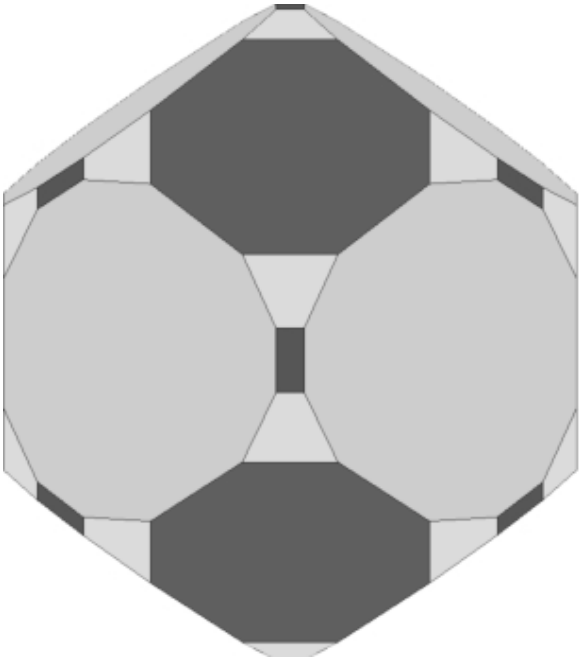

(d)

Fig. 7. (a) Photomicrograph of the ECS of a Pb-5at.%Bi-0.04at%Ni alloy cooled to a temperature where new facets have appeared at {311}, {530}, and {110} orientations [7]. (b) Photomicrograph of a partially equilibrated "negative" crystal of Bi-saturated Cu at 1223K, showing new facets at {110} and {320} [6]. (c) ECS of a Pb-5at.%Bi-0.08at%Ni alloy equilibrated at 548K for 13 hours; new facets have appeared at {110} and {210} orientations [7]. (d) Wulffman plot corresponding to (c), used to verify the orientations of the new facets.

pure crystals does not account for temperature (i.e. entropy) effects, and cannot therefore provide predictions of entropy-driven roughening. Thus, the prediction by the model of cusps at {111} and {100} orientations in pure FCC metals is consistent with the above measurements.

Studies of the ECS of pure Cu [16] at 1240K have shown that it also consists of predominantly

curved surfaces with small facets. However, in this case, facets occur not only at {111}, {100}, but also at {110} orientations. Thus, the simple nature of the NNBM does produce entirely satisfactory predictions for pure FCC metals. In contrast to the NNBM in the case of pure metals, the segregation model does account for some entropy effects, namely those associated with mixing of the components at the surface and in the bulk. Thus, where this entropy of mixing is significant compared with other surface entropy effects, the segregation model could provide some useful insights into the changes in ECS that arise in alloys due to surface segregation.

Only few experimental studies have been devoted to the ECS of alloys. As mentioned in the Introduction, studies of the ECS have been conducted on the Cu-O [5], Cu-Bi [6], and Pb-Bi-Ni [7] systems. In all these systems, completely faceted ECSs similar to those displayed in Fig. 6 have been found. The Cu-O system is not one that can be treated with the current model; however, it is useful to discuss some of the results obtained in the other two systems.

In the case of experiments on Pb containing Bi and Ni additions, the ECS was studied as a function of temperature [7]. At the highest temperatures, just below the melting point, the ECS of a Pb-5at.%Bi-0.04at.%Ni alloy was found to be similar to that of pure Pb, and to display small facets only at {111} and {100} orientations. Upon cooling, the first change in anisotropy manifested itself as an increase in {111}-facet size. This result is generally consistent with Fig. 3a, where the most significant surface energy decrease with decreasing temperature occurs for the {111} orientation. Upon further cooling, new facets appear simultaneously at {311} and {530} orientations. This interpretation of the results is based on a re-analysis of the original images using the Wulffman software [21]. The next new facet to form on the Pb alloy ECS, upon further temperature decrease, is the {110}. An image of the ECS, after the appearance of these new facets, is displayed in Fig. 7a. These results are qualitatively similar to the changes in the anisotropy of surface energy with decreasing temperature displayed on Fig. 3a, which shows new cusps developing at {311} and {110}. Although no new cusp is seen in Fig. 3a at {530}, one does appears at {210}, which lies only 4° away from {210} along the <100> zone.

Measurements of the ECS of Bi-saturated Cu were only performed at a temperature of 1223K [6]. In this case, the ECS was completely faceted (i.e. no curved surfaces were present) and displayed only {111}, {100}, {110}, and {320} facets, as shown in the partially equilibrated “negative” crystal displayed in Fig. 7b. The {320} orientation is also quite close to {210} (~7° along the <100> zone) at which a cusp is seen in Fig. 3a. One reason that the model may not predict the precise orientations at which new cusps are expected to form probably stems from its neglect of possible surface reconstruction effects. For example, in the case of Bi on Cu(100), the adsorbed Bi atoms can order into c(2X2), c($9\sqrt{2}$ X $\sqrt{2}$)R45° and p(10X10) structures [22-23] with increasing Bi coverage. These significant structural changes with increasing adsorption are presumably tied to the large size mismatch between Bi and the underlying Cu substrate. Thus, the level of adsorption on a surface of any given orientation will depend not only on the parameters included in the segregation model, but also on the ease with which mismatching segregated solute atoms can be accommodated on the template provided by the surface structure of the solvent (substrate). These structural effects may lead to surface configurations that differ in both adsorption and energy from those predicted by a model that does not account for interface reconstruction effects.

Finally, Fig. 7c shows the ECS of a Pb-5at.%Bi-0.08at.%Ni alloy equilibrated at 548K for 13 hours. Even though the Ni concentration of this alloy amounts merely to an increase from 400 to 800 ppm, in comparison to the alloy of Fig. 7a, the effects on the ECS are quite dramatic. In this case, a re-analysis of the crystal shape using the Wulffman software (shown in Fig. 7d) clearly identifies the new facets as {110} and {210}.

The above comparisons between model predictions and experimental results indicate that the surface segregation model may not include sufficient detail to allow quantitative predictions of the ECS of alloy crystals. Nevertheless it does provide qualitative predictions that can be useful in guiding the design of experiments and the interpretation of results. These include identification of a finite temperature range where facets other than {111} and {100} are likely to be found in experiments, and the importance of solute strain energy effects in driving the appearance of new facets in the ECS of FCC alloys.

ACKNOWLEDGEMENT

PW acknowledges with thanks support of his research by the MRSEC program of National Sci-

ence Foundation under grant DMR-0520425. DC wishes to thank the Agence Nationale de la Recherche for support of her research under grant ANR-REVMET-05-NT03-41834.

REFERENCES

[1] Y.W. Lee and H.I. Aaronson // *Surface Sci.* **95** (1980) 227.
[2] Y.W. Lee and H.I. Aaronson // *Acta Metall*. **28** (1980) 539.
[3] D.A. Steigerwald, S.J. Miller and P. Wynblatt // *Surface Sci.* **155** (1985) 79.
[4] P. Wynblatt and D. Chatain // Metall. Mater. *Trans.* **37A** (2006) 2595.
[5] E.D. Hondros and M. McLean, In: *Structures et Propriétés des Surfaces*, (Editions du CNRS: Paris, 1970), p. 219.
[6] D. Chatain, P. Wynblatt and G.S. Rohrer // *Acta Mater*. **53** (2005) 4057.
[7] W-C. Cheng and P. Wynblatt // *J. Crystal Growth* **173** (1997) 513.
[8] G. Wulff // *Z. Krist. Mineral* **34** (1901) 449.
[9] C. Herring, In: *Structure and Properties of Solid Surfaces*, edited by R.G. Gomer and C.S. Smith (University of Chicago Press: Chicago, 1953) p. 5.
[10] J.C. Heyraud and J.J. Metois // *Surface Sci.* **128** (1983) 334.
[11] K. Arenhold, S. Surnev, P. Coenen, H.P. Bonzel and P. Wynblatt // *Surface Sci.* **417** (1998) L1160.
[12] M. Nowicki, C. Bombis, A. Emundts, H.P. Bonzel and P. Wynblatt // *New J. Phys.* **4** (2002) 60.1
[13] J.C. Heyraud and J.J. Metois // *Acta Metall.* **28** (1980) 1789.
[14] J.C. Heyraud and J.J. Metois // *J. Crystal Growth* **50** (1980) 571.
[15] Z. Wang and P. Wynblatt // *Surface Sci.* **398** (1998) 259.
[16] D. Chatain, V. Ghetta and P. Wynblatt // *Interface Sci.* **12** (2004) 7.
[17] P. Wynblatt, A. Saůl and D. Chatain // *Acta Mater.* **46** (1998) 2337.
[18] J.D. Eshelby, In: *Progress in Solid Mechanics*, vol. 2, ed. by Sneddon and Hill (North-Holland: Amsterdam, 1961), p.275.
[19] J. Friedel // *Advan. Phys*. **3** (1954) 446.
[20] P. Wynblatt and R.C. Ku // *Surface Sci*. **65** (1977) 511.
[21] R. Roosen, R.P. McCormack and W.C. Carter // *Computational Mater. Sci*. **11** (1998) 16.
[22] H.L. Meyerheim, H. Zajonz, W. Moritz and I.K. Robinson // *Surface Sci.* **381** (1997) L551.
[23] H.L. Meyerheim, M. DeSantis, W. Moritz and I.K. Robinson // *Surface Sci.* **418** (1998) 295.